Imaging Microglia Surveillance during Sleep-wake Cycles in Freely Behaving Mice

Xiaochun Gu[2,3,7*#], Zhong Zhao[5,7#], Xueli Chen[7], Lifeng Zhang[7], Huaqiang Fang[7], Ting Zhao[8], Shenghong Ju[2], Weizheng Gao[6], Xiaoyu Qian[6], Xianhua Wang[4,7], Jue Zhang[6], Heping Cheng[1,4,7*]

1 National Biomedical Imaging Center, State Key Laboratory of Membrane Biology, Peking-Tsinghua Center for Life Sciences, College of Future Technology, Peking University, Beijing 100871, China

2 Jiangsu Key Laboratory of Molecular and Functional Imaging, Department of Radiology, Zhongda Hospital, Medical School, Southeast University, Nanjing 210009, China

3 Key Laboratory of Developmental Genes and Human Diseases, Department of Histology Embryology, Medical School, Southeast University, Nanjing 210009, China

4 State Key Laboratory of Membrane Biology, Beijing Key Laboratory of Cardiometabolic Molecular Medicine, Peking-Tsinghua Center for Life Sciences, Institute of Molecular Medicine, College of Future Technology, Peking University, Beijing 100871, China

5 Institute of Basic Medical Sciences Chinese Academy of Medical Sciences, School of Basic Medicine Peking Union Medical College, Beijing 100005, China

6 Academy of Advanced Interdisciplinary Study, College of Engineering, Peking University, Beijing 100871, China

7 Research Unit of Mitochondria in Brain Diseases, Chinese Academy of Medical Sciences, PKU-Nanjing Institute of Translational Medicine, Nanjing 211899, China

8 Nanjing Raygenitm Biotech Co., Ltd, Nanjing 211899, China

*Address correspondence to: chengp@pku.edu.cn, xiaochun.gu@seu.edu.cn

# These authors contributed equally to this work

Abstract

Microglia surveillance manifests itself as dynamic changes in cell morphology and functional remodeling. Whether and how microglia surveillance is coupled to brain state switches during natural sleep-wake cycles remain unclear. To address this question, we used miniature two-photon microscopy (mTPM) to acquire time-lapse high-resolution microglia images of the somatosensory cortex, along with EEG/EMG recordings and behavioral video, in freely-behaving mice. We uncovered fast and robust brain state-dependent changes in microglia surveillance, occurring in parallel with sleep dynamics and early-onset phagocytic microglial contraction during sleep deprivation stress. We also detected local norepinephrine fluctuation occurring in a sleep state-dependent manner. We showed that the locus coeruleus-norepinephrine system, which is crucial to sleep homeostasis, is required for both sleep state-dependent and stress-induced microglial responses and β_2-adrenergic receptor signaling plays a significant role in this process. These results provide direct evidence that microglial surveillance is exquisitely tuned to signals and stressors that regulate sleep dynamics and homeostasis so as to adjust its varied roles to complement those of neurons in the brain. *In vivo* imaging with mTPM in freely behaving animals, as demonstrated here, opens a new avenue for future investigation of microglia dynamics and sleep biology in freely behaving animals.

Introduction

Sleep is a highly conserved and essential phenomenon of the brain and serves numerous cognitive as well as metabolic and immunologic functions. Moreover, the sleep-wake transition represents a specific and prominent change in the brain state (Besedovsky et al., 2019; Rasch and Born, 2013). As compared to a wakeful brain, the sleeping brain shows more synchronous neuronal activities, which can be characterized by electroencephalography (EEG). Sleep has two main stages: the non-rapid eye movement (NREM) state, which is thought to promote clearance of metabolic waste partly through increased flow of interstitial fluid (Feng et al., 2019), and the rapid eye movement (REM) state, with EEG patterns similar to wakefulness yet with muscle atonia as well as vivid dreaming in humans (Besedovsky et al., 2019). In addition, sleep, especially NREM, is directly involved in memory consolidation (Fogel and Smith, 2011; Rasch and Born, 2013). However, the underlying biological dynamics and especially the cellular mechanisms of sleep regulation are not entirely understood (Frank, 2018; Frank and Heller, 2018).

Growing evidence shows that microglia dynamics are coupled to and intertwined with the sleep-wake cycle (Deurveilher et al., 2021; Hristovska et al., 2022). Microglia are resident innate immune cells ubiquitously distributed in the central nervous system and account for 10–15% of all brain cells (Wolf et al., 2017). Microglia surveillance refers to dynamic changes in cell morphology that accompany functional remodeling in response to changes in the neural environment (Liu et al., 2019; Nimmerjahn et al.,

2005; Stowell et al., 2019). It has been shown that microglia ablation disrupts the maintenance of wakefulness and promotes NREM sleep (Corsi et al., 2022; Liu et al., 2021), while enhancing an animal's fear memory consolidation (Wang et al., 2020). Conversely, acute and chronic sleep deprivation (SD) leads to microglia activation amidst a proinflammatory state triggered by elevated circulating levels of cytokines (C-reactive protein, TNF-α, IL-1, and IL-6) (Krueger et al., 2011). Thus, it is of critical interest to explore whether microglia surveillance can sense and respond to brain state changes during both natural sleep-wake cycles as well as under SD stress.

The investigation of microglial surveillance during the sleep-wake cycle demands technologies suitable to track the rapid dynamics of natural microglia behavior in real time. Though there have been pioneering studies on microglia dynamics in cultured brain slices (Honda et al., 2001), static *ex vivo* conditions can hardly recapitulate the dynamic microenvironments and neuronal activities *in vivo*. Based on results obtained from fixed brain slices, it has been shown that chronic sleep restriction but not acute sleep loss causes microglia process changes (Bellesi et al., 2017), but it is difficult to use this approach to reconstruct the dynamic behavior of microglia accurately and quantitatively. As a major advance, two-photon microscopy has recently been applied to image microglia in head-fixed or anesthetized animals, revealing microglial process motility, chemotaxis and homeostatic translocation, and multifaceted microglia-neuron interactions *in vivo* (Davalos et al., 2005; Eyo et al., 2018; Liu et al., 2019; Stowell et al., 2019). However, because of mechanical constraints or anesthetics, this technology

still precludes experimental paradigms in which natural sleep-wake cycle is undisturbed. In this regard, the recent advent of miniaturized two-photon microscopy (mTPM) has provided a powerful new tool ideal for fast and high-resolution brain imaging in freely behaving rodents (Zong et al., 2021, 2017). With the aid of mTPM, researchers have mapped the functional network topography of the medial entorhinal cortex (Obenhaus et al., 2022), deciphered the microcircuit dynamics in the dorsomedial prefrontal cortex during social competition (Zhang et al., 2022), and unraveled the specific itch signal processing in the primary somatosensory cortex (Chen et al., 2021).

In this study, we aimed to determine whether microglia surveillance undergoes any significant changes during natural sleep-wake cycles, and if so, what is the underlying regulatory mechanism. Using different models of mTPM tailored for high-resolution, multi-plane or large field-of-view (FOV) imaging, we monitored microglia in the somatosensory cortex of mice during natural sleep-wake cycles or while being subjected to acute SD. We found robust sleep state-dependent and SD-induced changes in microglia surveillance with characteristics differing from those induced by anesthetics. Furthermore, we showed that norepinephrine signals from the axonal projections of the locus coeruleus (LC) underlie the state-dependence of microglia surveillance and β_2-adrenergic receptor (β_2AR) signaling plays a significant role in this process.

Results

Imaging microglia dynamics in freely behaving mice

To visualize microglial morphology and dynamics during the sleep-wake cycle, microglia were specifically labeled with green fluorescent protein (GFP) expressed under the control of an endogenous Cx3cr1 promoter (Cx3cr1-GFP). Time-lapse imaging of the somatosensory cortex utilized the fast and high-resolution miniature two-photon microscope (FHIRM-TPM) recently developed by our laboratory (Zong et al., 2017), and EEG/Electromyography (EMG) signals and behavior videos were simultaneously recorded to determine corresponding sleep-wake states (Fig. 1a-c and Supplementary Fig. 1). The focal plane of the FHIRM-TPM was placed 50-100 μm beneath the surface of the somatosensory cortex with a field-of-view (FOV) of 220 × 220 μm (Fig. 1d). Under the experimental conditions, we were able to track morphological and positional changes of a cohort of 5-10 microglia at a frame rate of 5 frames per second (FPS) over prolonged durations of greater than 10 hours (Supplementary Fig. 1 and Video), while the animals were allowed to roam and behave freely and their sleep-wake cycles remained undisturbed. Though we were initially concerned with potential photoxicity associated with prolonged mTPM imaging, no changes in microglial morphology and fluorescent intensity were evident even after non-stop recording over the entire protocol period (Supplementary Fig. 1). This remarkable result indicates that photo damage is minimal, if any, during *in vivo* imaging (Supplementary Fig. 1).

Dynamic changes in microglial area, branching points, and process end-point speed were then analyzed using Imaris software (Fig. 1 e1-e3′ and Supplementary Fig. 1). We found that individual microglia maintained a relatively stable territory of surveillance over the entire experimental period, even while their individual projections extended and contracted incessantly, giving rise to a process end point motility of 1.39 ± 0.09 μm/min in the wake state (Fig. 1f-h). These results show that mTPM in conjunction with multi-modal recordings of EEG/EMG and behavioral videos enables *in vivo* visualization of microglia dynamics over multiple time scales in freely behaving mice. Interestingly, we also observed occasional short-range translocation in a few cells, suggesting the ability of microglia to survey territories beyond their own boundaries, in general agreement with recent observations in head-fixed mice (Eyo et al., 2018).

Microglia surveillance during the sleep-wake cycle

By simultaneously imaging microglia and recording EEG/EMG throughout a sleep-wake cycle, we obtained continuous 4-6 h datasets from different mice and, in conjunction with video interpretation, segmented and sorted them into subgroups corresponding to wake, NREM, and REM states (Fig. 2a). For each state we quantified morphological features and process motility from 15-20 cells. Wake and NREM states lasting longer than 1 min were identified, for which the last 30-seconds recording was selected, and REM states lasting longer than 30 seconds for the characterization of possible state-dependent microglia dynamic surveillance.

We found that during the NREM and REM states, microglial process length and surveillance area increased compared with those during wakefulness (Fig. 2b-d, b′-d′). Concomitantly, the number of branching points significantly increased, while end-point moving speed of microglial processes decreased (Fig. 2e-h), indicating state-dependent changes in microglial morphology as well as process motility under natural sleep-wake cycles. To provide a volumetric view of the dynamics of microglial morphology, we adapted our latest version of mTPM with an electrical tunable lens (ETL) capable of imaging variable focal planes (Fig. 2i-o and Supplementary Fig. 2) (Zong et al., 2021). Multi-plane reconstruction revealed more extended process lengths and greater branch point numbers as compared to single-plane imaging as expected (Fig. 2l, n). The volume of surveillance for individual microglia changed from 1661 ± 264.4 μm^3 in the wake state to 3802 ± 670.5 μm^3 in REM state and 4616 ± 324.6 μm^3 in NREM state (Fig. 2m). Similar to results obtained with single-plane imaging, the end-point speed of processes decreased in REM and NREM compared to the wake state (Fig. 2o). While both REM and NREM had the same trends in change as compared to the wake state, significantly greater changes were associated with NREM than REM in terms of cell volume, branch length, branch number, and end-point speed (Fig. 2l-o). These results demonstrate differential microglial dynamic surveillance as the brain state switches among wakefulness, REM and NREM, and the state-dependent morphological and process-motility changes can be robustly reproduced with either single-plane or volumetric imaging. Intriguingly, microglia can even sense and respond to subtle differences between REM and NREM states. Because more extended microglia are

171 thought to have greater surveillance ability (Kierdorf and Prinz, 2017), our results
172 support the notion that microglia during the NREM and REM periods tend to be more
173 active in the opportune clearing of metabolic wastes accumulated during the wake states.

174 To this end, it is also instructive to compare and contrast REM/NREM state-
175 dependent characteristics with those induced by anesthesia. In mice under isoflurane
176 (1.2% in air) for 20-30 min, we found that microglial length, area, number of branching
177 points (Supplementary Fig. 2) were similarly increased compared with the wake state,
178 as was the case in NREM and REM. However, the end-point movement of processes
179 exhibited opposite changes (Liu et al., 2019), increasing with anesthesia but decreasing
180 in sleep states (Fig. 2h, o and Supplementary Fig. 2). This result shows that microglia
181 surveillance appears to differ qualitatively between sleep and anesthesia states.

182

183 **Acute SD promotes contraction of microglial processes**

184 Sleep loss is detrimental to brain function and results in structural plastic changes
185 in nerve cells. Whether microglia dynamic surveillance alters after sleep loss remains
186 controversial (Bellesi et al., 2017; Wang et al., 2020). Therefore, we induced acute SD
187 in mice by forcing the animals to exercise and interrupting sleep with a rotatory rod,
188 starting at 9:00 am and lasting for six hours (zeitgeber time 2-8) **(**Fig. 3a**)**. The duration
189 of recovery sleep, especially NREM sleep, increased after SD (Supplementary Fig. 3).
190 In the wake state, microglia typically exhibited an extended form with ramified, long,

thin processes. Overt morphological changes occurred as early as 3h after SD, when microglia presented a contracted form bearing short and thick processes. By 6h, nearly all microglia cells were converted into a phagocytic form, assuming an amoeboid shape with few processes **(**Fig. 3b-d**)**. We found that microglial length, area and number of branching points decreased with the continuous SD (Fig. 3e-h). The same changes were observed in 3D reconstruction (Supplementary Fig. 3). Changes in the end-point speed of processes appeared to be biphasic, increasing at 3h SD and then declining below baseline level at 6h SD **(**Fig. 3h**)**; the latter may result in part from the dramatic shrinkage of the processes. As the sleep pressure was eased during recovery sleep, morphological changes of microglia were partially reversed over a timescale of several hours (Supplementary Fig. 3). Thus, our real-time recording in live animals clearly demonstrates that SD stress induces microglia to assume an active state and conspicuous microglial response occurs early in SD.

NE changes in somatosensory cortex during the sleep-wake cycle

Next, we sought to determine a possible signaling mechanism(s) that incites microglia surveillance state- and stress-dependent changes. Among a number of candidates responsible for stress responses, norepinephrine (NE) has recently been shown to play a crucial role in microglia surveillance by responding to neuronal network activity (Liu et al., 2019) and partaking of synaptic plasticity (Stowell et al., 2019). Therefore, we combined mTPM imaging with EEG and EMG recording to

212 determine whether NE levels in the somatosensory cortex fluctuate during the sleep-
213 wake cycle to control microglia surveillance. We imaged extracellular NE dynamics in
214 somatosensory cortical neurons with NE biosensor $GRAB_{NE2m}$ (Fig. 4a), which was
215 developed based on G protein receptors (Feng et al., 2019; Kjaerby et al., 2022). The
216 biosensor was expressed on the plasma membrane of neurons to report the dynamic
217 change of the extracellular NE. Dynamic changes of NE levels was evident in the
218 somatosensory cortex during wake, NREM and REM states (Fig. 4b). NE levels
219 reached higher levels during longer awakenings, while the lowest NE levels were
220 detected during REM sleep (Fig. 4b) and the largest changes in NE levels were recorded
221 occurred during the transition from REM to wake (Fig. 4b). During NREM sleep, the
222 NE oscillated dynamically around a relatively low level (Fig. 4b), with brief increases
223 that might be related to memory consolidation (Kjaerby et al., 2022). On average, mean
224 levels of NE exhibited a brain-state dependent change, varying in a decreasing order
225 from wake to NREM and to REM (Fig. 4c). These results are in general agreement with
226 recent observations that NE fluctuates in a sleep-state dependent manner in the medial
227 prefrontal cortex, and suggest that NE may play a crucial role in controlling the stage
228 dependent microglial changes.

229

230 **Role of the LC-NE signal in controlling the microglia dynamic surveillance**

231 To determine possible involvement of NE in sleep state- and SD-induced microglia
232 surveillance, we used the locus coeruleus (LC)-selective neurotoxin, N-(2-chloroethyl)-

n-ethyl-2-bromobenzylamine (DSP4; applied 2 days before imaging) to ablate LC axons projecting into the cortex (Supplementary Fig. 4) (Del C. González et al., 1998) and characterized microglial surveillance with and without an LC-NE signal (Fig. 5a). DSP4 application led to a significant increase in sleep states, particularly NREM sleep (Supplementary Fig. 4), in agreement with previous studies (Del C. González et al., 1998). Meanwhile, the characteristics of NE dynamics in different brain states were also changed by DSP4 (Supplementary Fig. 4). Importantly, the sleep state-dependent changes in microglia surveillance were abolished altogether; neither microglial morphology nor process motility displayed any of the previously significant changes seen when the brain states cycled across wake-REM-NREM (Fig. 5b-g). Likewise, DSP4 treatment completely prevented SD-induced alteration of microglia surveillance (Supplementary Fig. 4). These results indicate an essential role for the LC-NE signal in sleep- and stress-dependent state modulation of microglia surveillance.

The effects of the neural modulator NE are mediated by two families of G-protein-coupled receptors, α and β-adrenergic receptors (ARs), each comprising several subtypes and it has been shown that β_2AR stimulation rapidly induces microglia dynamic surveillance (Gyoneva and Traynelis, 2013; Liu et al., 2019; Stowell et al., 2019). We, therefore, examined microglia surveillance in β_2AR KO animals during natural sleep-wake cycles and under SD stress. Similar to LC axon ablation, β_2AR KO disturbed wake-sleep homeostasis, as manifested by a lengthening of overall sleep duration (Supplementary Fig. 4). By contrast, removal of β_2ARs failed to abolish

dynamic changes in microglia when the brain state switched between sleep and wakefulness (Fig. 5h-n). Nonetheless, the ability of microglia to subtly distinguish between REM and NREM states was largely compromised (Fig. 5h-n and Supplementary Fig. 4), suggesting a partial contribution of β_2AR signaling to LC-NE modulation of microglia surveillance during sleep-wake cycles. Regarding microglia responses to SD stress, we showed that microglial morphology and motility remained unchanged during the SD protocol in β_2AR KO animals (Supplementary Fig. 4), revealing a predominant role for β_2AR signaling in LC-NE modulation of microglia surveillance under SD stress.

Discussion

With the development of mTPM imaging and EEG/EMG recording in freely behaving mice, we now provide direct evidence that microglia surveillance in mouse somatosensory cortex is sleep-state dependent during natural sleep-wake cycles and that microglia contract from ramified into phagocytic forms a few hours after the onset of acute SD stress. Combined with pharmacological intervention and the use of NE biosensor and genetically manipulated animals, we showed that the LC-NE pathway mediates these state-dependent changes in microglia surveillance and that β_2AR signaling is involved in various aspects of the microglial responses, extending recent reports that the same pathway underlies microglia surveillance in the context of neuronal network activity (Liu et al., 2019) and synaptic plasticity (Stowell et al., 2019).

That microglia surveillance is sleep state-dependent substantiates an intimate relationship between rapid, robust state-dependent microglia remodeling and the biology of the sleep-wake cycle (Feng et al., 2019; Frank and Heller, 2018; Xie et al., 2013). It has been shown that microglia play a central role in the removal of metabolic waste and even cell debris from the brain (Huisman et al., 2022; Márquez-Ropero et al., 2020). Our study shows that microglia in the sleeping brain have larger area and length, consistent with greater clearance ability in the sleeping state than the waking. Recently, it has been reported that, in head-fixed mice, microglial morphological complexity was decreased in NREM sleep than during wakefulness (Hristovska et al.,

2022). In consideration of the altered durations of both NREM and REM sleep (Hristovska et al., 2022), the unnatural sleep state would lead to an increase in the microarousal state, and ultimately lead to a change in the structure of the sleep state, which may be the main reason for the difference in microglia behavior from our natural sleep. Furthermore, our results show that microglia surveillance significantly differs between REM and NREM sleep in the somatosensory cortex, likely reflecting metabolic and functional differences between the two states. More specifically, previous reports have proposed differential roles between the NREM and REM sleep for consolidation of different types of memories. For example, NREM sleep contributes to declarative memories, whereas REM sleep is important for procedural and emotional memories (Besedovsky et al., 2019; Rasch and Born, 2013). Memory consolidation is closely related to synaptic plasticity, in which microglia play a very important role (Corsi et al., 2022; Tuan and Lee, 2019). In this regard, our findings hint at the possibility that not all features of microglia-neuron interactions, including mode of action and localization, are equal in the consolidation of different types of memory.

It has been shown that a large proportion of Iba1-immunoreactive microglia with larger cell bodies and less ramified processes appear in hippocampal brain slices following 48-72h of sleep deprivation and in the frontal cortex after 4.5 days of chronic sleep restriction, whereas acute sleep deprivation for 8 hours had no effect on microglial morphology (Bellesi et al., 2017; Hall et al., 2020). However, these findings have

mostly been derived from slice staining. While the present work support the general conclusion that microglia surveillance is responsive to SD stress, our real-time mTPM imaging *in vivo* also unmasked a progressive change in microglia surveillance that occurred as early as 3h after onset of SD and full conversion of microglia into the phagocytic form after 6h SD stress. This apparent disparity between the current and previous reports might reflect the complications arising from *ex vivo* sample preparation, because microglia surveillance is highly dynamic and sensitive to neural environmental changes, evidenced by its cyclic changes during the sleep-wake switch.

We have provided two lines of evidence that the LC-NE-β_2AR axis is involved in microglial surveillance both during natural sleep-wake cycle and under SD stress. Ablation of LC-NE neuronal projection abolished and knockout of β_2ARs markedly altered the manifestation of the state-dependence of microglia surveillance, while the latter recapitulated most, but not all, the phenotypes of the former. These findings are well supported by emerging evidence that NE is necessary for microglial activation (Bellesi et al., 2016; Berridge et al., 2012). First, NE is known to be a key neurotransmitter that regulates sleep dynamics (Wang et al., 2020) and the dynamics of microglia (Liu et al., 2019; Sugama et al., 2019). Second, it has been shown β_2AR expressed at higher level in microglia than other CNS cell types (Zhang et al., 2014) and microglia dynamic surveillance rapidly responds to β_2AR stimulation (Gyoneva and Traynelis, 2013; Liu et al., 2019; Stowell et al., 2019). Moreover, the morphology of microglia in somatosensory cortex is also regulated by neuronal activity, in a

326 microglial β_2AR-dependent manner (Liu et al., 2019). Our results also extend the
327 classic view of NE regulation of sleep and wakefulness by revealing a prominent
328 microglial component in the NE response. It should be noted that pan-tissue β_2AR
329 knockout animal model was used in the current study and it warrants future
330 investigation to pinpoint specific roles of microglial β_2AR in the brain-state dependent
331 microglial responses.

332 In addition to NE, other potential modulators also present dynamic during sleep-
333 wake cycle and may partake in the regulation of microglia dynamic surveillance. It has
334 been reported that LC firing stops (Aston-Jones et al., 1981; Rasmussen et al., 1986),
335 while inhibitory neurons, such as PV neurons and VIP neurons, become relatively
336 active during REM sleep (Brécier et al., 2022). ATP level in basal forebrain is shown to
337 be higher in REM sleep than NREM sleep (Peng et al., 2023). Similarly, adenosine level
338 in the somatosensory cortex during REM sleep is higher than in NREM sleep (Response
339 figure 1). These considerations may explain the finding that β_2AR knockout failed to
340 abolish microglial responses to sleep state switch and SD stress altogether. A more
341 complete understanding of the regulatory mechanisms of microglia surveillance will
342 help to delineate more precisely roles of microglia in physiology and under stress.

343 In summary, by real-time *in vivo* mTPM imaging of microglia surveillance, we
344 uncovered the state-dependence of microglia surveillance during natural sleep-wake
345 cycles and a robust, early-onset response to SD stress. Both types of microglial
346 dynamics are under the regulation of LC-NE with the involvement of β_2ARs as one of

its main effectors. These results highlight that microglia undergo rapid and robust remodeling of both morphology and function to fulfill multimodal roles complementary to those of neurons in the brain. In addition, the methodologies established in the present study may prove to be of broad application for future investigations of microglia dynamics and sleep biology in freely behaving animals.

Acknowledgements

We thank Dr. Wei Xie from Southeast University and Dr. Hailan Hu from Zhejiang University for their carefully reading and valuable comments; Li Wang and Tong Zhu from Raygenitm Biotech Co., Ltd, and Ying Guo from the company Transcend Vivoscope for comments on the optics, biological experiments, and data processing; and the Nanjing Brain Observatory for data processing services. The work was supported by grants from the National Science and Technology Innovation 2030 Major Program (2021ZD0202200, 2021ZD0202205, 2022ZD0211900 and 2022ZD0211903), the National Natural Science Foundation of China (32293210, 92157105, 31971158, 81827809, 81827805, 82130060 and 61821002), CAMS Innovation Fund for Medical Sciences (2019-I2M-5-054), National Key Research and Development Program (2018YFA0704100 and 2018YFA0704104), Jiangsu Provincial Medical Innovation Center (CXZX202219), Collaborative Innovation Center of Radiation Medicine of Jiangsu Higher Education Institutions, Nanjing Life Health Science and Technology

Project (202205045), and Key Core Technology Research Project for Nanjing Enterprise Academician Workstation.

Author contributions

X.G. and H.C. conceived the project and supervised the research; X.G. designed and supervised the biological experiments. X.G., Z.Z. and X.C. performed the experiments and led data analysis and figure-making; X.Q. and W.G. contributed data analysis under the supervision of H.C., J.Z., and X.G; X.G. and H.C. wrote the manuscript with inputs from L.Z. and H.F., while all authors participated in discussions and data interpretation.

Competing interests

The authors declare no competing interests.

Methods

Animals

All experimental protocols were carried out with the approval of the Institutional Animal Care and Use Committee of PKU-Nanjing Institute of Translational Medicine (Approval ID: IACUC-2021-023). Male mice, 2-3 months of age, were used in accordance with institutional guidelines. Cx3cr1-GFP (Jax, #021160) heterozygous

mice were used to visualize microglia with miniature two-photon microscopy (mTPM). To ablate LC-NE neurons, DSP4 (Sigma, #C8417) solution was administered intraperitoneally (50 mg/kg) twice at 24-h intervals and a minimum of 48 h before mTPM imaging. Adrb2 KO (Jax, #031496) mice were crossed with Cx3cr1-GFP mice to generate (Cx3cr1-GFP+/-; Adrb2-/-) mice, which were used in experiments with β_2-adrenergic receptor knock-out. Mice were housed with a standard 12h light/12h dark cycle and fed standard chow *ad libitum*.

Surgery and electrode implantation

All surgical procedures were done sterilely, and all animal-administered reagents were sterile. Mice were anesthetized with isoflurane (1.5% in air at a flow rate of 0.4 L/min) and maintained on a 37°C heating pad during surgery. The cerebral cortical region to be imaged was localized based on the stereotactic coordinates (somatosensory area, from bregma: anteroposterior, -1 mm, mediolateral, +2 mm) and marked with a fine black dot. The skull over the region of interest was thinned with a high-speed micro-drill under a dissection microscope. Drilling and application of normal saline were done intermittently to avoid overheating and hurting the underlying cerebral tissue. After removing the external layer of the compact bone and most of the spongy bone layer with the drill, the area continued to thinned until an expanded smooth area (~3 mm in diameter) was achieved, making sure the middle was thin enough to get high quality imaging. A drop of saline was applied and a 3-mm-diameter glass coverslip previously sterilized in 70% ethanol was placed on this window, then dental cement was applied

around the glass coverslip. The mice were used in the experiment after 4 weeks of postoperative recovery.

500 nL of AAV9-hSyn-GRAB$_{NE2m}$ (BrainVTA, #PT-2393) were injected into the somatosensory cortex (A/P, -1 mm; M/L, +2 mm; D/V, -0.3mm) at a rate of 50 nL/min. 3-mm-diameter glass coverslip were implanted and fixed on the somatosensory cortex. The mice were used in the experiment one month after postoperative recovery.

Epidural screw electrodes (diameter 0.8 mm) were implanted bilaterally on the opposite sides of the imaging window for constant EEG recording from the frontal (bregma: anteroposterior, +1.5 mm, mediolateral, +1.5 mm) and parietal cortex (anteroposterior, -2 mm; mediolateral, +2.5 mm). Electrodes were fixed to the skull with dental cement. Another pair of electrodes was inserted into the neck muscles for EMG recording. Then, a headpiece baseplate was attached to the skull with cyanoacrylate and reinforced with dental cement.

Simultaneous imaging and recording

After recovery from surgery, mice with a clear cranial window and typical EEG/EMG signals were selected for further experiments. With the mice head-fixed on the imaging stage, an mTPM imaging stack was first acquired using an mTPM (Transcend Vivoscope), and a proper field-of-view (FOV) with 5-10 microglial somata was located 50-100 μm beneath the pial surface. The holder of the mTPM was then sealed onto the baseplate over the coverslip on the head, and the mTPM could be repetitively mounted

and dismounted to track the same population of microglia over different days (Supplementary Fig. 1).

Three models of mTPM were used for different experiments: FHIRM-TPM high-resolution model (Zong et al., 2017) with lens NA of 0.7 and FOV of 220 × 220 μm for Figs. 1-5; headpiece weight was 2.13 g, and lateral and axial resolutions were 0.74 and 6.53 μm, respectively. FHIRM-TPM large FOV model (Zong et al., 2021) with a headpiece weight of 2.45 g, lens NA of 0.5, and FOV of 420 × 420 μm for Supplementary Fig. 4, and lateral and axial resolutions were 1.13 and 12.2 μm, respectively; FHIRM-TPM 2.0 ETL model (Zong et al., 2021) in Supplementary Fig. 2, with headpiece weight of 4.3 g, Z-depth range of 45 μm, lens NA of 0.7, lateral resolution of 0.74 μm, axial resolution of 6.53 μm, and FOV of 220 x 220 μm. Images were acquired to visualize the microglial surveillance: time-lapse xy imaging stack at a frame rate of 5 FPS or multi-plane imaging stacks (20 planes at 2 μm intervals, 5 frames/s). Each model of mTPM was equipped with a water-immersion miniature objective and a 920 nm femtosecond fiber laser. Excitation for fluorescence imaging was achieved with 150-fs laser pulses (80 MHz) at 920 nm for GFP with a power of ~25 mW after the objective.

The EEG/EMG signals were recorded continuously and simultaneously by Vital Record (Kissei Comtec system), and mouse behavior was monitored with an infrared video camera. Mice were never disturbed when they were undergoing spontaneous sleep-wake cycles, feeding, or drinking.

Sleep deprivation

Sleep deprivation (SD) was achieved by forcing the mice to move continuously through power devices (Soft maze, #XR-XS108) (Pandi-Perumal et al., 2007). The experimental device consisted of a computer console, a horizontal rotating rod with a diameter of 46 cm and a round mouse cage of 50 cm. The rotating rod can rotate horizontally randomly (3 times/min) in clockwise and counterclockwise directions under the control of the computer. The mouse was placed in the cage one hour per day for one week for habituation. After baseline sleep recording, mice were sleep-deprived for the duration indicated in each experiment, starting at 9:00 AM and lasting up to 6h into SD.

Anesthesia experiment

Time-lapsed image stacks acquired between 20 and 30 min after anesthesia (isoflurane, 1.5% in air at a flow rate of 0.4 L/min) were used to evaluate microglial dynamic surveillance under anesthetized conditions.

Quantification and statistical analysis

EEG/EMG data analysis

EEG and EMG signals were amplified and filtered as follows: EEG, high-pass filter at 0.1 Hz, low-pass filter at 35 Hz; and EMG, high-pass filter at 10 Hz, low-pass filter at 100 Hz. All signals were digitalized at 128 Hz and stored on a computer. As described previously (Bellesi et al., 2013), EEG power spectra were computed by a fast Fourier

transform routine for 10 s epochs. Wake, nonrapid eye movement (NREM) sleep, and REM sleep were manually scored off-line (SleepSign, Kissei Comtec) in 10 s epochs according to standard criteria (Fogel and Smith, 2011). Epochs containing artifacts, predominantly during animal movement, were excluded from spectral analysis.

Microglial Morphological Analysis

In order to accurately quantify microglial morphometric changes in different brain states, wake and NREM states lasting longer than 1 min were chosen, among which the last 30 seconds of recording was selected, in conjunction with video interpretation, for further processing and analysis. Because they were of relatively short duration, REM states lasting longer than 30 seconds were used for analysis.

Image stacks were first processed offline using ImageJ software to correct for xy motion artifacts, and the time-lapse stack was aligned using the StackReg plugin. In some experiments, motion artifacts due to Z-level drift was further minimized by collecting multi-plane images over ±20 μm depth at 2 μm intervals and then compressing them into a single xy projection to substitute for time-lapsed xy image. In this case, corresponding projections were generated over a 30-seconds window to substitute for time-lapsed xy images. A maximum-intensity projection (MIP) was then created from the stack for morphological analysis. The criteria to select microglia for analysis included a clearly identifiable soma and processes seen in the x-y plane.

Next, microglial morphological analysis was done using Imaris 9.5 software and the Filament module (Supplementary Fig. 1). The filament created in Imaris is a connected graph-based object consisting of vertices that are connected by edges. Feature extraction by the Filament module yielded microglial features and parameters defined as the following:

Microglial process: Same a filament dendrite in module. Microglial processes form the main structure of the filament object. Processes extend from the microglial cell body and can undergo branching. A process graph is a sequence of vertices connected by edges.

Number of branch points: Same a filament branch depth in module. The process graph is a tree-based structure that has a root point. Branching depth is defined as the number of branches or bifurcations in the shortest path from the beginning point to a given point in the process graph.

Process length: Same a filament dendrite length in module, in reference to the sum of all process lengths within the entire microglial cell.

Microglial surveillance area: Same a filament dendrite area in module, in reference to the sum of all process areas within the entire microglial cell.

Microglial surveillance volume: Same as filament dendrite volume. In volumetric imaging, it is the sum of the volumes of all processes within the microglial cell.

Process end-point speed: Same as filament track speed. The speed is calculated using the "Track over time" function and given by the absolute track length change, whether extension or retraction, divided by the corresponding elapsed time.

NE signals analysis

To analyze NE signals data, we binned the raw data into 1 Hz and subtracted the background autofluorescence. $\Delta F/F_0$ were calculated by using the fluorescence signal itself. F_0 was defined as the mean value of the lowest fluorescence signal for each 60-second window in each recorded fluorescence signal. The z-score transformed $\Delta F/F_0$ was used for analysis. In order to accurately quantify the changes of NE signals in different brain states, wake and NREM states with a duration of more than 1 min were selected, in which the mean value of 30 seconds fluorescence signal at the end was selected as the NE signal in this state, which was further processed and analyzed combined with video interpretation. Since the duration of REM state is relatively short and it enters a low level at the end of REM, the mean value of fluorescence signal in the 30s before the transition from REM state to wake state is used to represent NE signal in REM state.

Statistical analyses

Significance levels indicated are as follows: $^{*}P < 0.05$, $^{**}P < 0.01$, $^{***}P < 0.001$. All data are presented as mean±SEM. All statistical tests used were two-tailed. Statistical

527 significance was determined using both parametric (ANOVA) and non-parametric
528 (Friedman) tests with post-hoc. All statistical testing was performed using GraphPad
529 Prism 6.0 (GraphPad Software). No statistical methods were used to predetermine
530 sample sizes, but our sample sizes were similar to those reported in previous
531 publications (Davalos et al., 2005; Nimmerjahn et al., 2005).
532

References

Aston-Jones G, Bloom FE. 1981. Activity of norepinephrine-containing locus coeruleus neurons in behaving rats anticipates fluctuations in the sleep-waking cycle. *J Neurosci* **1**:876–886. doi:10.1523/JNEUROSCI.01-08-00876

Bellesi M, De Vivo L, Chini M, Gilli F, Tononi G, Cirelli C. 2017. Sleep loss promotes astrocytic phagocytosis and microglial activation in mouse cerebral cortex. *J Neurosci* **37**:5263–5273. doi:10.1523/JNEUROSCI.3981-16.2017

Bellesi M, Pfister-Genskow M, Maret S, Keles S, Tononi G, Cirelli C. 2013. Effects of sleep and wake on oligodendrocytes and their precursors. *J Neurosci* **33**:14288–14300. doi:10.1523/JNEUROSCI.5102-12.2013

Bellesi M, Tononi G, Cirelli C, Serra PA. 2016. Region-specific dissociation between cortical noradrenaline levels and the sleep/wake cycle. *Sleep* **39**:143–154. doi:10.5665/sleep.5336

Berridge CW, Schmeichel BE, España RA. 2012. Noradrenergic modulation of wakefulness/arousal. *Sleep Medicine Reviews* **16**:187–197. doi:10.1016/j.smrv.2011.12.003

Besedovsky L, Lange T, Haack M. 2019. The sleep-immune crosstalk in health and disease. *Physiological Reviews* **99**:1325–1380. doi:10.1152/physrev.00010.2018

Brécier A, Borel M, Urbain N, Gentet LJ. 2022. Vigilance and behavioral state-dependent modulation of cortical neuronal activity throughout the sleep/wake cycle. *J Neurosci* **42**:4852–66. doi: 10.1523/JNEUROSCI.1400-21.2022

Chen X-J, Liu Y-H, Xu N-L, Sun Y-G. 2021. Multiplexed representation of itch and mechanical and thermal sensation in the primary somatosensory cortex. *J Neurosci* **41**:10330–10340. doi:10.1523/JNEUROSCI.1445-21.2021

Corsi G, Picard K, di Castro MA, Garofalo S, Tucci F, Chece G, del Percio C, Golia MT, Raspa M, Scavizzi F, Decoeur F, Lauro C, Rigamonti M, Iannello F, Ragozzino DA, Russo E, Bernardini G, Nadjar A, Tremblay ME, Babiloni C, Maggi L, Limatola C. 2022. Microglia modulate hippocampal synaptic transmission and sleep duration along the light/dark cycle. *Glia* **70**:89–105. doi:10.1002/glia.24090

Davalos D, Grutzendler J, Yang G, Kim JV, Zuo Y, Jung S, Littman DR, Dustin ML, Gan W-B. 2005. ATP mediates rapid microglial response to local brain injury in vivo. *Nat Neurosci* **8**:752–758. doi:10.1038/nn1472

Del C. González MM, Debilly G, Valatx J-L. 1998. Noradrenaline neurotoxin DSP-4 effects on sleep and brain temperature in the rat. *Neuroscience Letters* **248**:93–96. doi:10.1016/S0304-3940(98)00333-4

568 Deurveilher S, Golovin T, Hall S, Semba K. 2021. Microglia dynamics in sleep/wake
569 states and in response to sleep loss. *Neurochem Int* **143**:104944.
570 doi:10.1016/j.neuint.2020.104944

571 Dworak M, McCarley RW, Kim T, Kalinchuk AV, Basheer R. 2010. Sleep and brain
572 energy levels: ATP changes during sleep. *J Neurosci* **30**:9007–9016.
573 doi:10.1523/JNEUROSCI.1423-10.2010

574 Eyo UB, Mo M, Yi M-H, Murugan M, Liu J, Yarlagadda R, Margolis DJ, Xu P, Wu L-
575 J. 2018. P2Y12R-dependent translocation mechanisms gate the changing microglial
576 landscape. *Cell Reports* **23**:959–966. doi:10.1016/j.celrep.2018.04.001

577 Feng J, Zhang C, Lischinsky JE, Jing M, Zhou J, Wang H, Zhang Y, Dong A, Wu Z,
578 Wu H, Chen W, Zhang P, Zou J, Hires SA, Zhu JJ, Cui G, Lin D, Du J, Li Y. 2019.
579 A genetically encoded fluorescent sensor for rapid and specific in vivo detection of
580 norepinephrine. *Neuron* **102**:745-761.e8. doi:10.1016/j.neuron.2019.02.037

581 Fogel SM, Smith CT. 2011. The function of the sleep spindle: a physiological index of
582 intelligence and a mechanism for sleep-dependent memory consolidation.
583 *Neuroscience & Biobehavioral Reviews* **35**:1154–1165.
584 doi:10.1016/j.neubiorev.2010.12.003

585 Frank MG. 2018. The role of glia in sleep regulation and function In: Landolt H-P, Dijk
586 D-J, editors. Sleep-Wake Neurobiology and Pharmacology, Handbook of
587 Experimental Pharmacology. Cham: Springer International Publishing. pp. 83–96.
588 doi:10.1007/164_2017_87

589 Frank MG, Heller HC. 2018. The function(s) of sleep In: Landolt H-P, Dijk D-J, editors.
590 Sleep-Wake Neurobiology and Pharmacology, Handbook of Experimental
591 Pharmacology. Cham: Springer International Publishing. pp. 3–34.
592 doi:10.1007/164_2018_140

593 Gyoneva S, Traynelis SF. 2013. Norepinephrine Modulates the Motility of Resting and
594 Activated Microglia via Different Adrenergic Receptors. *Journal of Biological*
595 *Chemistry* **288**:15291–15302. doi:10.1074/jbc.M113.458901

596 Hall S, Deurveilher S, Robertson GS, Semba K. 2020. Homeostatic state of microglia
597 in a rat model of chronic sleep restriction. *Sleep* **43**:zsaa108.
598 doi:10.1093/sleep/zsaa108

599 Honda S, Sasaki Y, Ohsawa K, Imai Y, Nakamura Y, Inoue K, Kohsaka S. 2001.
600 Extracellular ATP or ADP induce chemotaxis of cultured microglia through $G_{i/o}$ -
601 coupled P2Y receptors. *J Neurosci* **21**:1975–1982. doi:10.1523/JNEUROSCI.21-
602 06-01975.2001

603 Hristovska I, Robert M, Combet K, Honnorat J, Comte J-C, Pascual O. 2022. Sleep
604 decreases neuronal activity control of microglial dynamics in mice. *Nat Commun*
605 **13**:6273. doi:10.1038/s41467-022-34035-9

606 Huisman Y, Uphoff K, Berger M, Dobrindt U, Schelhaas M, Zobel T, Bussmann J, Van
607 Impel A, Schulte-Merker S. 2022. Meningeal lymphatic endothelial cells fulfill
608 scavenger endothelial cell function and cooperate with microglia in waste removal
609 from the brain. *Glia* **70**:35–49. doi:10.1002/glia.24081

610 Kierdorf K, Prinz M. 2017. Microglia in steady state. *Journal of Clinical Investigation*
611 **127**:3201–3209. doi:10.1172/JCI90602

612 Kjaerby C, Andersen M, Hauglund N, Untiet V, Dall C, Sigurdsson B, Ding F, Feng J,
613 Li Y, Weikop P, Hirase H, Nedergaard M. 2022. Memory-enhancing properties of
614 sleep depend on the oscillatory amplitude of norepinephrine. *Nat Neurosci*
615 **25**:1059–1070. doi:10.1038/s41593-022-01102-9

616 Krueger JM, Majde JA, Rector DM. 2011. Cytokines in immune function and sleep
617 regulation. Handbook of Clinical Neurology. Elsevier. pp. 229–240.
618 doi:10.1016/B978-0-444-52006-7.00015-0

619 Liu H, Wang X, Chen Lu, Chen Liang, Tsirka SE, Ge S, Xiong Q. 2021. Microglia
620 modulate stable wakefulness via the thalamic reticular nucleus in mice. *Nat*
621 *Commun* **12**:4646. doi:10.1038/s41467-021-24915-x

622 Liu YU, Ying Y, Li Y, Eyo UB, Chen T, Zheng J, Umpierre AD, Zhu J, Bosco DB, Dong
623 H, Wu L-J. 2019. Neuronal network activity controls microglial process
624 surveillance in awake mice via norepinephrine signaling. *Nat Neurosci* **22**:1771–
625 1781. doi:10.1038/s41593-019-0511-3

626 Márquez-Ropero M, Benito E, Plaza-Zabala A, Sierra A. 2020. Microglial corpse
627 clearance: lessons from macrophages. *Front Immunol* **11**:506.
628 doi:10.3389/fimmu.2020.00506

629 Mori K, Ozaki E, Zhang B, Yang L, Yokoyama A, Takeda I, Maeda N, Sakanaka M,
630 Tanaka J. 2002. Effects of norepinephrine on rat cultured microglial cells that
631 express α1, α2, β1 and β2 adrenergic receptors. *Neuropharmacology* **43**:1026–1034.
632 doi:10.1016/S0028-3908(02)00211-3

633 Nimmerjahn A, Kirchhoff F, Helmchen F. 2005. Resting microglial cells are highly
634 dynamic surveillants of brain parenchyma in vivo. *Science* **308**:1314-8.
635 doi:10.1126/science.1110647

636 Obenhaus HA, Zong W, Jacobsen RI, Rose T, Donato F, Chen L, Cheng H, Bonhoeffer
637 T, Moser M-B, Moser EI. 2022. Functional network topography of the medial

entorhinal cortex. *Proc Natl Acad Sci USA* **119**:e2121655119. doi:10.1073/pnas.2121655119

Pandi-Perumal SR, Cardinali DP, Chrousos GP. 2007. Neuroimmunology of sleep. New York, NY: Springer.

Peng W, Liu X, Ma G, Wu Z, Wang Z, Fei X, Qin M, Wang L, Li Y, Zhang S, Xu M. 2023. Adenosine-independent regulation of the sleep–wake cycle by astrocyte activity. *Cell Discov* **9**:16. doi:10.1038/s41421-022-00498-9

Rasch B, Born J. 2013. About sleep's role in memory. *Physiological Reviews* **93**:681–766. doi:10.1152/physrev.00032.2012

Rasmussen K, Morilak DA, Jacobs BL. 1986. Single unit activity of locus coeruleus neurons in the freely moving cat: I. During naturalistic behaviors and in response to simple and complex stimuli. *Brain Research* **371**:324–334. doi:10.1016/0006-8993(86)90370-7

Stowell RD, Sipe GO, Dawes RP, Batchelor HN, Lordy KA, Whitelaw BS, Stoessel MB, Bidlack JM, Brown E, Sur M, Majewska AK. 2019. Noradrenergic signaling in the wakeful state inhibits microglial surveillance and synaptic plasticity in the mouse visual cortex. *Nat Neurosci* **22**:1782–1792. doi:10.1038/s41593-019-0514-0

Sugama S, Takenouchi T, Hashimoto M, Ohata H, Takenaka Y, Kakinuma Y. 2019. Stress-induced microglial activation occurs through β-adrenergic receptor: noradrenaline as a key neurotransmitter in microglial activation. *J Neuroinflammation* **16**:266. doi:10.1186/s12974-019-1632-z

Tuan L-H, Lee L-J. 2019. Microglia-mediated synaptic pruning is impaired in sleep-deprived adolescent mice. *Neurobiology of Disease* **130**:104517. doi:10.1016/j.nbd.2019.104517

Wang C, Yue H, Hu Z, Shen Y, Ma J, Li J, Wang X-D, Wang Liang, Sun B, Shi P, Wang Lang, Gu Y. 2020. Microglia mediate forgetting via complement-dependent synaptic elimination. *Science* **367**:688–694. doi:10.1126/science.aaz2288

Wolf SA, Boddeke HWGM, Kettenmann H. 2017. Microglia in physiology and disease. *Annu Rev Physiol* **79**:619–643. doi:10.1146/annurev-physiol-022516-034406

Xie L, Kang H, Xu Q, Chen MJ, Liao Y, Thiyagarajan M, O'Donnell J, Christensen DJ, Nicholson C, Iliff JJ, Takano T, Deane R, Nedergaard M. 2013. Sleep drives metabolite clearance from the adult brain. *Science* **342**:373–377. doi:10.1126/science.1241224

Zhang C, Zhu H, Ni Z, Xin Q, Zhou T, Wu R, Gao G, Gao Z, Ma H, Li H, He M, Zhang J, Cheng H, Hu H. 2022. Dynamics of a disinhibitory prefrontal microcircuit in

673 controlling social competition. *Neuron* **110**:516-531.e6.
674 doi:10.1016/j.neuron.2021.10.034

675 Zhang Y, Chen K, Sloan SA, Bennett ML, Scholze AR, O'Keeffe S, Phatnani HP,
676 Guarnieri P, Caneda C, Ruderisch N, Deng S, Liddelow SA, Zhang C, Daneman R,
677 Maniatis T, Barres BA, Wu JQ. 2014. An RNA-sequencing transcriptome and
678 splicing database of glia, neurons, and vascular cells of the cerebral cortex. *J*
679 *Neurosci* **34**:11929–11947. doi:10.1523/JNEUROSCI.1860-14.2014

680 Zong W, Wu R, Chen S, Wu J, Wang H, Zhao Z, Chen G, Tu R, Wu D, Hu Y, Xu Y,
681 Wang Y, Duan Z, Wu H, Zhang Y, Zhang J, Wang A, Chen L, Cheng H. 2021.
682 Miniature two-photon microscopy for enlarged field-of-view, multi-plane and long-
683 term brain imaging. *Nat Methods* **18**:46–49. doi:10.1038/s41592-020-01024-z

684 Zong W, Wu R, Li M, Hu Y, Li Y, Li J, Rong H, Wu H, Xu Y, Lu Y, Jia H, Fan M, Zhou
685 Z, Zhang Y, Wang A, Chen L, Cheng H. 2017. Fast high-resolution miniature two-
686 photon microscopy for brain imaging in freely behaving mice. *Nat Methods*
687 **14**:713–719. doi:10.1038/nmeth.4305

688

Figures

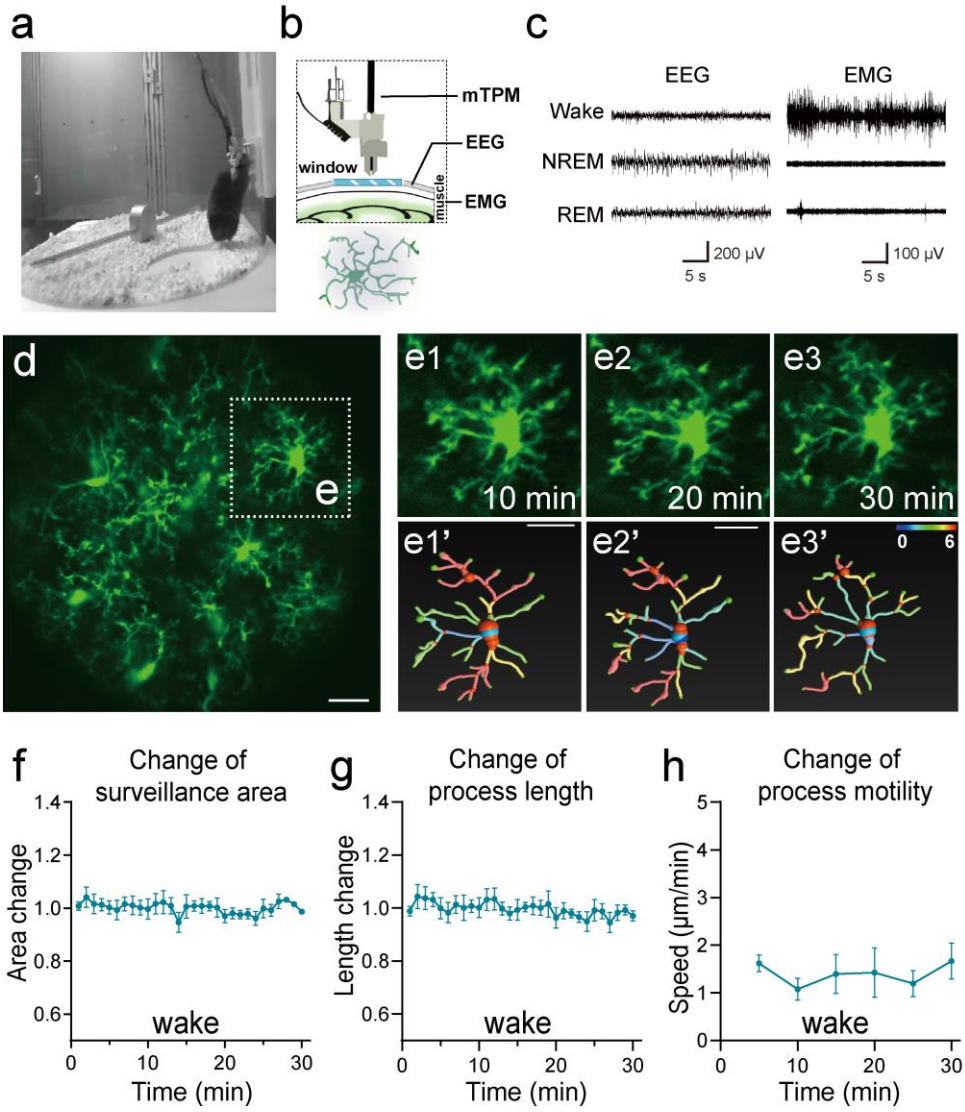

Fig. 1. Imaging microglial surveillance in the somatosensory cortex in freely moving mice.

(a-c) Experimental setup. The animal was head-mounted with a miniature two-photon microscope (mTPM) and EEG/EMG electrodes and behaved freely in a cylindrical chamber (a). Microglia expressing GFP in the somatosensory cortex were imaged through a cranial window using the mTPM (b) and the sleep/wake state of the animal was simultaneously monitored using an EEG/EMG recording system (b-c).

(d-e) Microglial morphological dynamics when the animal was awake. A representative image with a FOV of 220 × 220 μm^2. **(e1-e3)** Expanded views of selected microglia in

box from (d) at 10 min (e1), 20 min (e2) and 30 min (e3) of continuous recording. **(e1'-e3')** Microglial process graphs digitally reconstruction for E1-E3 using Imaris software. In Figure e1′-e3′, the branch points of processes are represented in red and the number of different branches of the whole cell is represented as gradient colors.

(f-h) Quantitative analysis of changes in microglia surveillance area (f), process length (g), and process motility, indexed by the speed of the extension and retraction at end points of the processes (h). Note that the gross morphology of microglia remained largely unchanged over a 30-min time frame in the wake state, despite significant motility at the ends of the processes. Scale bars, 25 μm.

n = 12 cells from 3 mice. Scale bars, 30 μm. See supplementary Fig. 1-3 for more details.

The online version of this article includes the following video, source data, and figure supplement(s) for figure 1:

Source Data 1. Imaging microglial surveillance in the somatosensory cortex in freely moving mice.

Figure Supplement 1. Microglia dynamics imaging and analysis in freely behaving mice.

Figure 1-video 1. Imaging data of a 1-hour continuous recording of somatosensory cortex in a freely behaving mouse. The frame rate of image acquisition was 5 Hz. Raw data with 10-frame averaging.

Figure 1-video 2. Correction for xy motion artifacts.

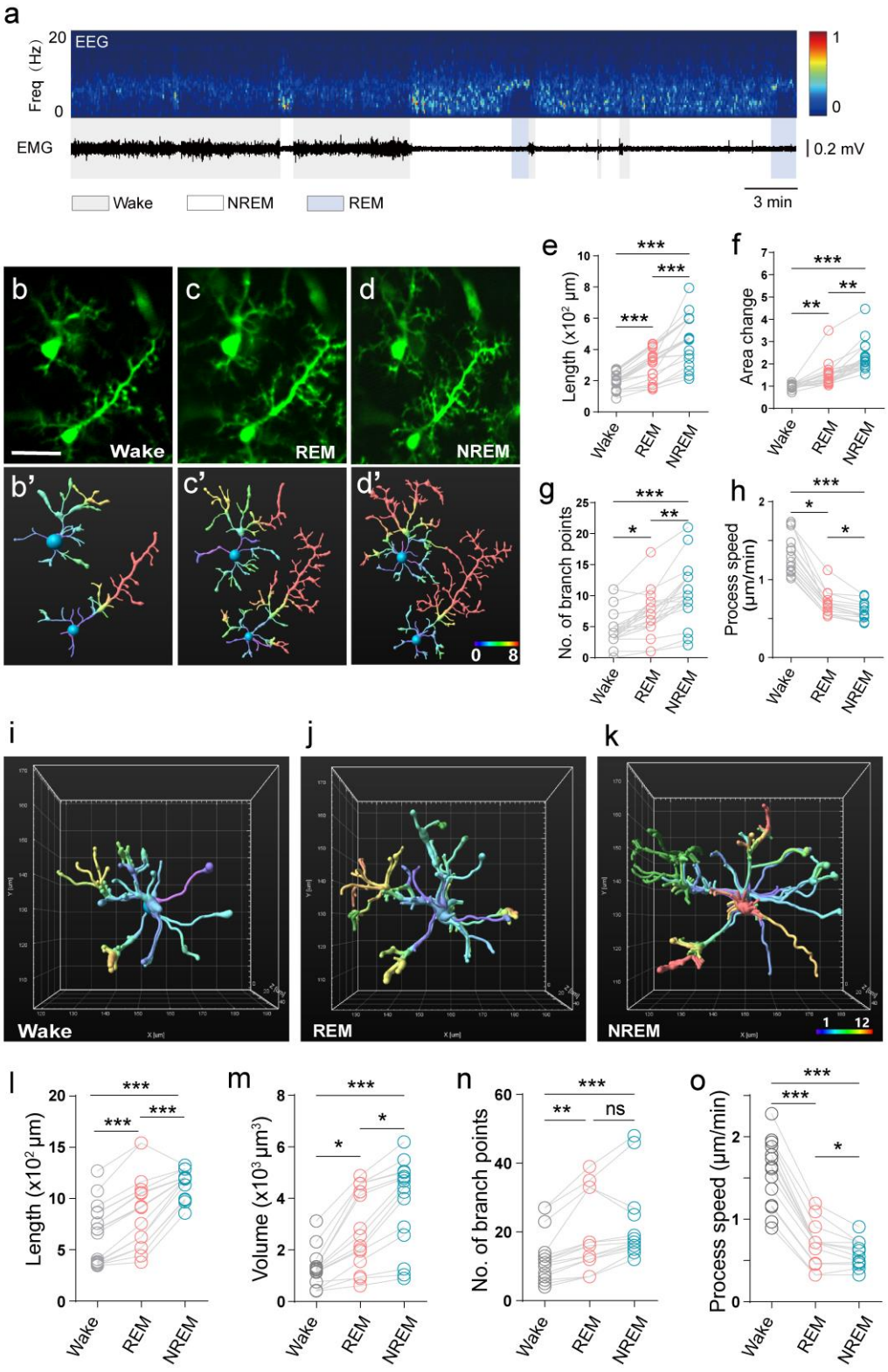

Fig. 2. Microglial surveillance is state-dependent in the sleep-wake cycle.

(a) Representative EEG/EMG recordings showing the sleep-wake stage switch. Top,

726 EEG power spectrogram (1-20 Hz). Middle, EMG trace. Bottom, brain states classified
727 as wake (color code: gray), REM (blue), and NREM (white).

728 **(b-d)** Representative microglial morphological changes during the sleep-wake cycle.
729 **(b′-d′)** Microglial morphology reconstructed from b-d using Imaris software.

730 **(e-h)** Microglial morphological parameters, length (e), area change (f), number of
731 branch points (g), and process end point speed (h), all exhibited brain state-dependent
732 dynamic change.

733 One-way ANOVA with Tukey's post-hoc test in **e**; Friedman test with Dunn's post-hoc
734 test in **f-h**; $n = 20$ cells from 7 mice for each group (**e-g**), $n = 15$ cells from 6 mice for
735 each group (**h**); $^{*}P < 0.05$, $^{**}P < 0.01$, $^{***}P < 0.001$.

736 **(i-o)** 3D multi-plane imaging and reconstruction of microglial morphology. A 3D ETL
737 lens was used to acquire multi-plane imaging (220*220*40 μm^3) at Z-intervals of 2 μm,
738 at a rate of 7.5 stacks/5 min.

739 **(i-k)** 3D reconstructed microglial morphology in wake (i), REM (j), and NREM (k)
740 states, with corresponding time stamps shown at the bottom.

741 **(l-o)** Quantitative analysis of microglial length (l), volume change (m), number of
742 branch points (n), and process motility (o) based on multi-plane microglial imaging.
743 Data from 3D imaging corroborated state-dependent changes of microglial morphology
744 in the sleep-wake cycle. Scale bars, 30 μm.

745 One-way ANOVA with Tukey's post-hoc test in **l, o**; Friedman test with Dunn's post-
746 hoc test in **m, n**; $n = 17$ cells from 7 mice for each group (**l-n**), $n = 15$ cells from 6 mice
747 for each group (**o**); $^{*}P < 0.05$, $^{**}P < 0.01$, $^{***}P < 0.001$.

748

749 The online version of this article includes the following source data and figure
750 supplement(s) for figure 2:

751 **Source Data 1.** Microglial surveillance is state-dependent in the sleep-wake cycle.

752 **Figure Supplement 2.** Multiplane imaging of microglial surveillance and changes of
753 microglial surveillance under anesthesia.

754

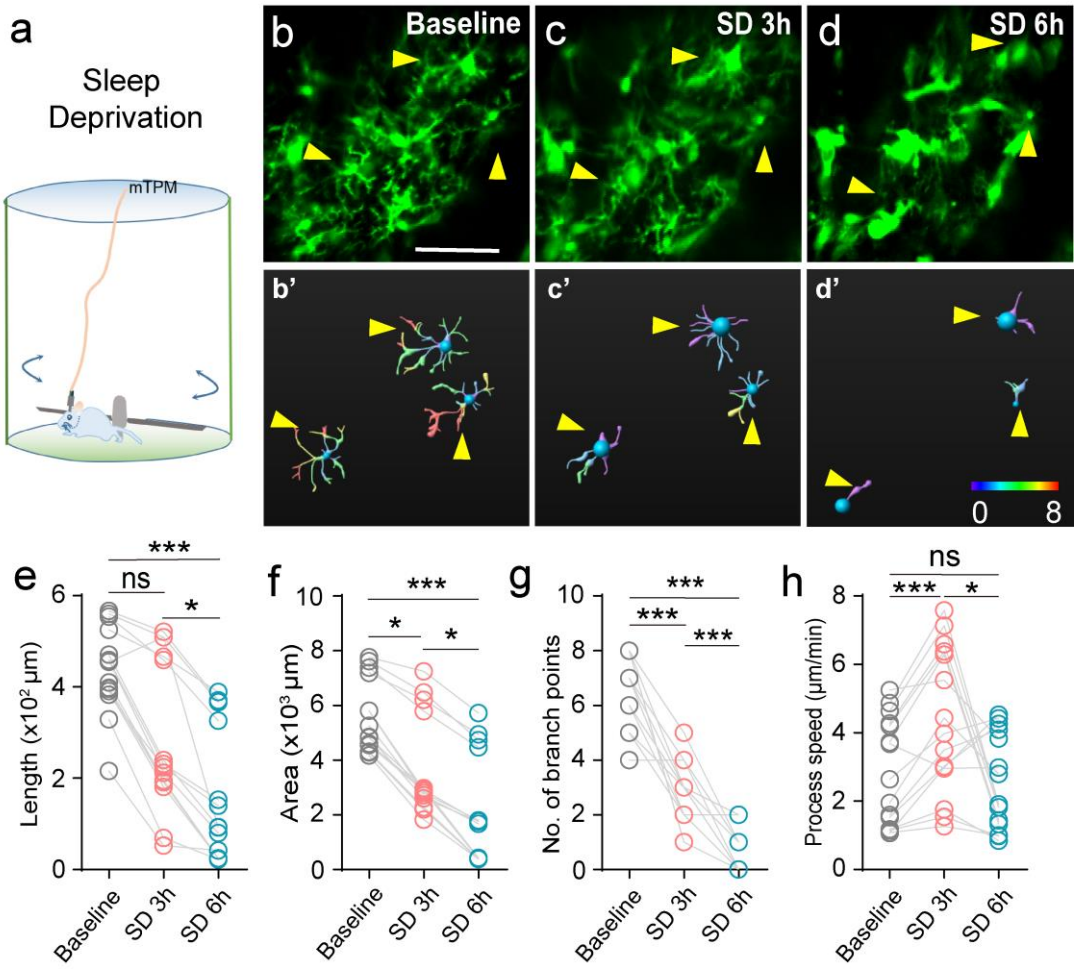

Fig. 3. Changes of microglial surveillance in the state of sleep deprivation.

(a) Experimental setup for sleep deprivation. Sleep deprivation in mice was achieved by forcing them to exercise and interrupting their sleep with the rotation of a 46-cm rod (18 turns/min) in the chamber (diameter 50 cm).

(b-d) Microglial processes contracted after sleep deprivation (SD), baseline (b), SD 3h (c), and SD 6h (d). (b′-d′) Morphological changes of microglia reconstructed using Imaris software. b'-d' correspond to b-d, respectively.

(e-h) Statistics for length (e), area (f), number of branch points (g), and process motility (h). Scale bar, 30 μm.

One-way ANOVA with Tukey's post-hoc test in **g, h**; Friedman test with Dunn's post-hoc test in **e, f**; $n = 15$ cells from 6 mice for each group; $*P < 0.05$, $***P < 0.001$.

The online version of this article includes the following source data and figure supplement(s) for figure 3:

Source Data 1. Changes of microglial surveillance in the state of sleep deprivation.

Figure Supplement 3. Changes of microglial surveillance in the state of sleep deprivation and recovery.

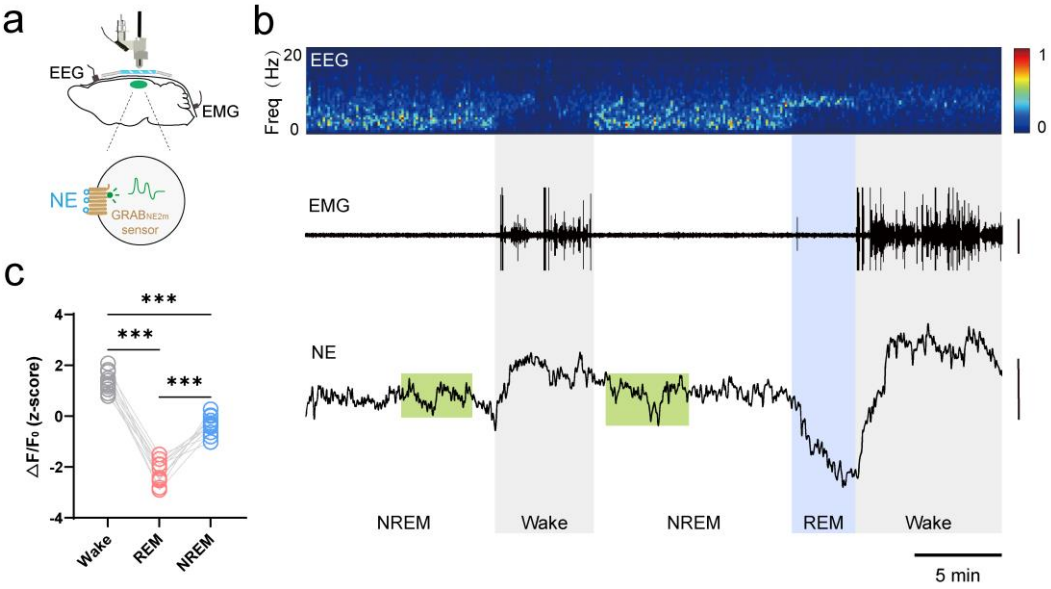

Fig. 4. NE dynamics in mouse somatosensory cortex during the sleep-wake cycle.

(a) Schematic diagram depicting mTPM recording of extracellular NE indicated by the $GRAB_{NE2m}$ sensor expressed in neurons.

(b) Representative traces of simultaneous recordings in the somatosensory cortex during the sleep-wake cycle in freely behaving mice. EEG and its power spectrogram (0-20 Hz); EMG (scale, 50 μV); NE signals reflected by the z-score of the $GRAB_{NE2m}$ fluorescence (scale, 2 z-score). The brain states are color-coded (wake, gray; NREM, white; REM, blue; NE oscillatory during NREM sleep, green).

(c) Mean extracellular NE levels in different brain states. Data from the same recording are connected by lines. ***$P < 0.001$, one-way ANOVA with Tukey's post-hoc test (n = 11 from 3 mice).

The online version of this article includes the following source data for figure 4:

Source Data 1. NE dynamics in mouse somatosensory cortex during the sleep-wake cycle.

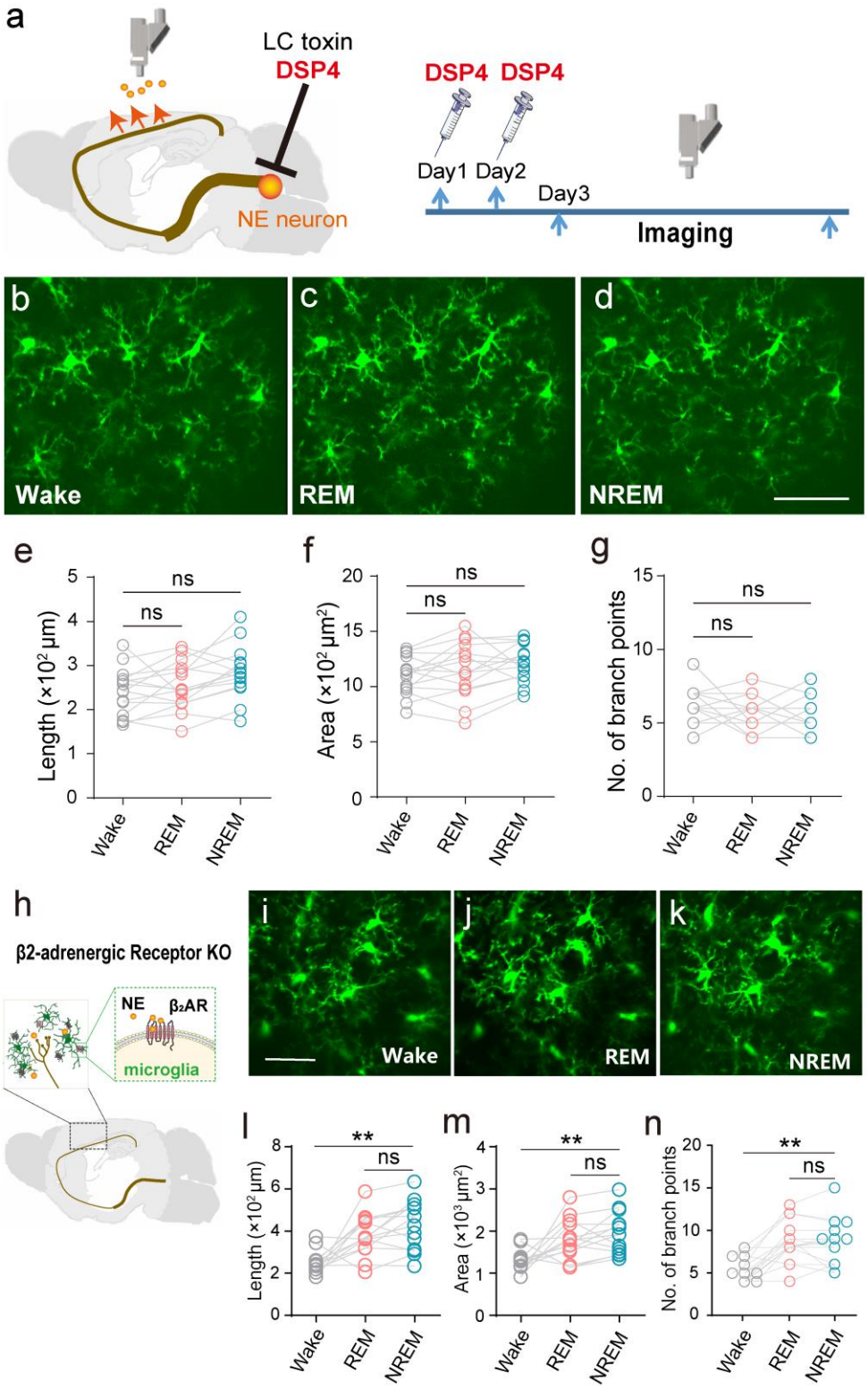

Fig. 5. Microglial surveillance during natural sleep is controlled by LC-NE signal.

(a) Experimental setup: LC-selective neurotoxin DSP4 was used to destroy LC-NE neuronal axons.

(b-g) Lack of sleep/wake state-dependent microglial surveillance in LC- axon ablated animals. b-d: Representative mTPM images of microglia at different states. e-g: Statistics for microglial length (e), surveillance area (f), and number of branch points (g) in LC-axon ablated mice.

One-way ANOVA with Tukey's post-hoc test in **e, f**; Friedman test with Dunn's post-hoc test in **g**; n = 15 cells from 6 mice for each group; ns, not significant.

(h) Schematic diagram for β_2ARs on the plasma membrane of microglia in the cerebral cortex responding to NE released from axonal terminals projected from LC.

(i-k) State-dependent microglial surveillance during sleep-wake cycle in β_2AR knockout mice. Representative microglial images (i-k) and statistics for microglial process length (l), surveillance area (m), and number of branch points (n) at different states in (CX3CR1-GFP+/-; Adrb2-/-) mice. Scale bar, 30 μm.

One-way ANOVA with Tukey's post-hoc test in **m**; Friedman test with Dunn's post-hoc test in **l, n**; n = 15 cells from 6 mice for each group; ns, not significant, $^{**}P < 0.01$.

The online version of this article includes the following source data and figure supplement(s) for figure 5:

Source Data 1. Microglial surveillance during natural sleep is controlled by LC-NE signal.

Figure Supplement 4. Altered sleep-wake states after DSP4 administration and β2AR knockout and controlling microglial surveillance during SD by LC-NE signal.